

RESEARCH ARTICLE | AUGUST 25 2023

Mechanism of antifreeze protein functioning and the “anchored clathrate water” concept **FREE**

Jan Zielkiewicz  



J. Chem. Phys. 159, 085101 (2023)

<https://doi.org/10.1063/5.0158590>



View
Online



Export
Citation

CrossMark

Articles You May Be Interested In

Structure of solvation water around the active and inactive regions of a type III antifreeze protein and its mutants of lowered activity

J. Chem. Phys. (August 2016)

Comparative analysis of hydration layer reorientation dynamics of antifreeze protein and protein cytochrome P450

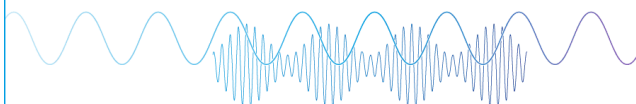
Chinese Journal of Chemical Physics (June 2022)

A two-dimensional adsorption kinetic model for thermal hysteresis activity in antifreeze proteins

J. Chem. Phys. (May 2006)

Webinar

Boost Your Signal-to-Noise
Ratio with Lock-in Detection



Sep. 7th – Register now



Zurich
Instruments

Mechanism of antifreeze protein functioning and the “anchored clathrate water” concept

Cite as: J. Chem. Phys. 159, 085101 (2023); doi: 10.1063/5.0158590

Submitted: 17 May 2023 • Accepted: 4 August 2023 •

Published Online: 25 August 2023



View Online



Export Citation



CrossMark

Jan Zielkiewicz^{a)} 

AFFILIATIONS

Faculty of Chemistry, Department of Physical Chemistry, Gdańsk University of Technology, Narutowicza 11/12, 80-233 Gdańsk, Poland

^{a)} Author to whom correspondence should be addressed: jan.zielkiewicz@pg.edu.pl

ABSTRACT

In liquid water, there is a natural tendency to form aggregates that consist of water molecules linked by hydrogen bonds. Such spontaneously formed aggregates are surrounded by a “sea” of disordered water molecules, with both forms remaining in equilibrium. The process of creating water aggregates also takes place in the solvation water of proteins, but in this case, the interactions of water molecules with the protein surface shift the equilibrium of the process. In this paper, we analyze the structural properties of the solvation water in antifreeze proteins (AFPs). The results of molecular dynamics analysis with the use of various parameters related to the structure of solvation water on the protein surface are presented. We found that in the vicinity of the active region responsible for the binding of AFPs to ice, the equilibrium is clearly shifted toward the formation of “ice-like aggregates,” and the solvation water has a more ordered ice-like structure. We have demonstrated that a reduction in the tendency to create “ice-like aggregates” results in a significant reduction in the antifreeze activity of the protein. We conclude that shifting the equilibrium in favor of the formation of “ice-like aggregates” in the solvation water in the active region is a prerequisite for the biological functionality of AFPs, at least for AFPs having a well-defined ice binding area. In addition, our results fully confirm the validity of the “anchored clathrate water” concept, formulated by Garnham *et al.* [Proc. Natl. Acad. Sci. U. S. A. **108**, 7363 (2011)].

Published under an exclusive license by AIP Publishing. <https://doi.org/10.1063/5.0158590>

PROLEGOMENA

Since the discovery of antifreeze proteins (AFPs) more than half a century ago, their functioning is still of great interest to many researchers. A widely accepted explanation is that these proteins adsorb permanently¹⁻³ on the surface of a spontaneously formed embryo/ice crystal and, thus, prevent further ice growth at the adsorption site. Consequently, the surface of ice growing between the adsorption sites becomes curved. According to the Gibbs–Thomson effect, the melting temperature of a convex surface is lower than that of a flat one. Due to this phenomenon, the ice formation eventually stops at a certain temperature range. Because a key step of the described mechanism is the adsorption of protein onto ice, the intriguing question arises as to how AFP, being surrounded by liquid water, recognizes the ice surface and adsorbs onto it. It is surprising that effective recognition is performed despite the absence of any chemical differences between water and ice. Furthermore, both liquid water and ice display strong structural similarity due to the presence of a tetrahedral network of hydrogen bonds, and

thus, the structural differences between these two phases are very subtle. Kristiansen and Zachariassen⁴ postulated that the adsorption process occurs in two stages. First, the adsorption site solidifies (that is, the solvation layer in the active region of the protein surface solidifies), which is accompanied by the formation of a distinct crystal plane. Only then does AFP bind to this newly formed surface. According to the authors, adsorption is not possible without the formation of an ice layer. The binding is possible because of the specific structure of the active region on the surface of AFP (ice-binding surface, IBS), where both the flat shape and the specific arrangement of the hydrophilic and hydrophobic groups play an important role in creating the molecule’s affinity for ice. This suggests that the solvation layer in the active region (IBS) of AFP must be specifically arranged in order to transform into ice. This finding is supported by the fact that the solvation water of the “ordinary” surface of a protein molecule does not freeze,⁵⁻⁷ and consequently, such a protein surface is repelled from the ice crystal plane. The concept of the specific ordering of solvation water in the vicinity of IBS has been confirmed by various authors,^{8,9} who noted a significant degree of

structural ordering in the water layer located in the vicinity of IBS in AFPs. This finding suggests the occurrence of an ice-like structure in this particular layer of water. In addition, the analysis of solvation water dynamics leads to a similar conclusion.^{10–12} All of the above seems to indicate the formation of an ice-like motif, which links the IBS of AFP to ice. Later on, Garnham *et al.*¹³ proposed the concept of “anchored clathrate water” (ACW), which had been based on x-ray crystallographic images of the interaction between *MpAFP* and ice at 100 K. According to this concept, anchored clathrate water binds to the IBS of AFP in positions that fit into the crystal lattice of ice. Thus, it can be said that an AFP molecule brings its own “ice”¹⁴ on its active surface in the form of pre-structured ice-like water molecules, which are anchored to the protein’s surface, supporting the crystallization of the surrounding water. It is noteworthy that other authors also found a very similar arrangement of hydration water molecules in the vicinity of IBS of *LpAFP*¹⁵ and *TisAFP*.¹⁶

Although the concept of ACW is soundly based on previous observations, i.e., significant structural ordering of solvation water in the vicinity of IBS, its veracity has been questioned by Hudait *et al.*¹⁷ Based on the results of molecular simulations, the authors stated that the solvation water in the active region of *TmAFP* does not exhibit ice- or ACW-like order in solution. The ACW motif forms only when *TmAFP* migrates into the vicinity of the ice surface and positions itself in an orientation optimal for binding to it. According to the authors, these findings strongly suggest that the initial ordering of the solvation water layer is not necessary for the recognition of ice by AFP. In addition, the studies on the hyperactive AFPs showed that these proteins do not induce (in aqueous solution) pre-ordering of water molecules in the solvation layer of AFP’s active region into ice-like structures.^{18–21} This finding supports the conclusion, reached by Hudait *et al.*, that the ordered water structure required for ACW formation is only induced when the synergy between AFP and the ice crystal surface occurs. Such interpretation is also supported by the fact that the solvation layer of ice spreads over a distance on the order of 1 nm,^{22–24} and the initial stages of the adsorption process depend on the interactions between the solvation layers of a protein and ice.^{25–27}

As the brief review above clearly indicates, the solvation of the IBS of AFP differs significantly from the pattern characterizing other proteins. The notion that this specific solvation pattern is essential for AFP to perform its antifreeze function is widely accepted in the literature. However, there are two reasons for which the acceptance of the concept of ice-like ordering of water adjacent to the IBS is highly controversial. First, different authors have different understanding of the term “ice-like structure” in relation to solvation water. The need for clarification has already been recognized by Nemethy and Scheraga, who wrote: “Thus, although the term ‘ice-like’ was used in describing the clusters, it referred only to the extent of hydrogen bonding and did not necessarily imply that the clusters have the tridymite-like arrangement of ordinary ice. The latter is merely one of several possible, nearly equivalent structures although it might be expected to occur quite often, especially at low temperatures, in analogy with ice, because it offers a relatively large number of hydrogen bonds for a given cluster size. It is to be noted that rather irregular arrangements of the molecules in the clusters are not excluded by the model as the clusters do not extend beyond a few molecular diameters. Thus there is no need to confine the possible structures to long range repeating arrangements, a weak point

of some semicrystalline structural theories for water.”²⁸ The second reason is the high structural lability of the liquid phase, which obviously hampers the detection of any structural motifs (and found to be ice-like).

Thus, we now wish to clarify how we understand an increase in the structural order of solvation water and what can/should be considered its “ice-like structure.” This will allow us to reach two goals, i.e., to avoid the aforementioned controversy and to show that, with such a clarification, the concept of an “anchored clathrate” is absolutely correct. Moreover, in this paper, we demonstrate that the existence of such a clathrate is a prerequisite for AFPs to perform their function. Below, we present arguments that will justify the proposed thesis in regard to the model describing the structure of liquid water.

Liquid water exhibits unusual thermodynamic properties that distinguish it from other molecular liquids. The most well-known anomalies are the lower density of ice compared to liquid water and the occurrence of a density maximum at 4 °C. Other thermodynamic parameters of water, for example, the isothermal compressibility coefficient (κ) or heat capacity (c_p), also show a remarkable temperature dependence. To explain these anomalies, Tanaka published²⁹ a model describing the structure of liquid water. The model assumes that there are two types of structural ordering in liquid water, characterized by two independent order parameters. The first type is translational ordering, tending toward the tightest possible spatial packing of molecules in the liquid, where the liquid density is a measure of ordering. The second type is orientational ordering, resulting from the directional properties of hydrogen bonding. It manifests itself in the tendency to maintain a preferred spatial arrangement and mutual orientation of water molecules. This mechanism naturally counteracts the increase in density due to the resulting spatially ordered structures of considerable volume. Tanaka assumed (as Nemethy and Scheraga²⁸ did at one time) that “locally favored structures” are formed in liquid water. They are aggregates made of water molecules connected by hydrogen bonds that are energetically stable and with a significant volume of their own. In this paper, we use the term HVA (high volume aggregates) in order to abbreviate the notation and to emphasize the most characteristic property of these structures. HVAs occur in the liquid in relatively small amounts, being surrounded by a “sea” of disordered water molecules that form a phase of greater than average density. At first glance, the presented idea may resemble the concept of the coexistence of two phases characterized by different densities (high density amorphous phase, HDA, and low density amorphous phase, LDA)³⁰ in liquid water. However, it is not identical, as pointed out by Tanaka.²⁹ According to the author, the parameter describing the degree of orientational ordering of water is equivalent to the content of HVAs in liquid water. The presence of high volume aggregates plays a key role in the freezing of water.³¹

Thus, in liquid water, an equilibrium is established, which determines the relative content of two structural forms: HVA and disordered phase. The values of various physicochemical parameters of water (e.g., density, viscosity, and compressibility) depend on the equilibrium point. A legitimate question arises here about the structure of postulated aggregates, but Tanaka’s model does not provide a clear answer. Some of the most likely candidates are six-membered rings or the so-called octameric units.^{32,33} It is noteworthy that the aforementioned structures are configurational elements of

hexagonal ice. Obviously, these are not the only possible solutions. For example, five-membered rings, whose presence in the liquid phase is responsible for the ability of liquid water to transition into a glassy state,^{34,35} are another option.

The equilibrium point mentioned above depends on temperature but not exclusively. It is to be expected that it will also depend on the interactions between liquid water and the surface of a solute molecule (such as protein). If the distribution of hydrophilic atoms on the surface of a solute molecule is “matched” to the spatial arrangement of water molecules in HVA, then the aggregate will only weakly recognize the vicinity of the solvated surface. However, if the hydrophilic atoms are arranged on the surface of solute in a chaotic manner (as is probably the case with most proteins), then HVAs will get disorganized via interactions with this surface. This is the explanation, presented by us previously,³⁶ of the well-known observation about the increased water density in the solvation layer of proteins. We demonstrated that HVAs are destructed in the vicinity of the protein surface, which results in an increase in water density. This effect applies to most proteins. However, in the vicinity of IBS in AFP, the equilibrium between the two structural forms of liquid water is shifted in the direction of strengthening the tendency to form HVAs.

Distinct behavior of solvation water at the IBS is attributed to two factors that occur simultaneously. First, it is the hydrophobic nature of IBS. It is thought³⁷ that the significant degree of hydrophobicity of this area (together with its flat shape) ensures the functioning of AFP. According to the well-known concept of “icebergs” by Frank and Evans,³⁸ water around the hydrophobic functional groups, such as CH₃, is characterized by increased degree of ordering. This results in the formation of pseudocrystalline structures (“icebergs”). Although Frank and Evans’ concept was considered very controversial for many years, we have recently confirmed its validity using the results of molecular simulations.³⁹ We demonstrated that water molecules connected by hydrogen bonds form ice-like aggregates in the solvation layer of model hydrophobic substances. We also showed that the formation of these aggregates is more likely to occur in the solvation layer of solutes than in bulk water. It has been easy to relate these observations to the IBS of AFP since the active surface of AFP has a pronounced hydrophobic character (attributed to the protruding CH₃ groups). Thus, a similar enhancing effect due to the presence of HVA should be expected here as well. The second important factor is the distribution of hydrophilic groups (for example, OH) on the IBS. The distribution “matches” the spatial distribution of water molecules in HVAs. This creates favorable conditions not only for anchoring of HVA to the IBS but also for its additional stabilization. It is noteworthy that the existence of such anchoring of HVA to the IBS in CfAFP was already demonstrated in our previous work⁷ (see Fig. 4 thereof). During the freezing process, HVAs present in the solvation water are transformed into the fragments of the crystal lattice of ice.

The argumentation presented above allows us to clarify the concept of “ice-like structure” of solvation water as one that contains more HVA than bulk water at the same temperature.

Based on the presented considerations, the following solvation model of the IBS of AFP emerges. In liquid water, energetically stable high-volume HVAs, consisting of water molecules bonded by hydrogen bonds, form spontaneously. These aggregates occur in the

liquid in relatively small amounts, remaining in equilibrium with a “sea” of disordered water molecules, which form a phase of above-average density. In the case of solvation water, the equilibrium point depends on how water molecules interact with the surface of a solute. Interaction with the “ordinary” surface of protein generally shifts the equilibrium toward the HVA destruction. The opposite scenario occurs in the vicinity of IBS where the equilibrium shifts toward the HVA formation. Moreover, formed HVAs have the ability to bind to the IBS due to the specific structure of the latter. As we will show later in this paper, water molecules binding to the IBS prefer to occupy specific positions in space, and the structural ordering of solvation water around the IBS is ice-like in the sense described above. Therefore, we believe that the existence of an equivalent of ACW in the liquid phase is possible. At the same time, it seems more relevant to use the term “fluent clathrate”²⁷ instead of “anchored clathrate” because both the preferred positions of water molecules and the structure of solvation water are largely blurred. Since the process of water freezing proceeds through a gradual reorganization of the liquid structure toward the formation and merging of HVA structures,^{32,40} it can be stated that the HVAs “anchored” to the IBS provide specific crystallization nuclei for nascent hexagonal ice. Increasing the number of these nuclei in the vicinity of IBS facilitates the transformation of liquid water into a solid phase (ice), while their anchoring to this surface is responsible for the process of adsorption of an AFP to ice.

The described model was used by us previously²⁷ to present the interaction between CfAFP and ice. The model explains the possibility of “remote” interaction with the ice surface as well as the characteristic “periodic” profile (as a function of distance) of the potential energy curve for this interaction. It also explains very a similar “periodic” profile of the potential energy curve for the interaction between the IBS of two RiAFP molecules in water.⁴¹ Additionally, the model has been confirmed by the observation of a different but functionally similar class of proteins, that is, ice nucleation proteins (INPs). For this group of proteins, the structure of active region is very similar to that observed in the hyperactive AFPs.⁴² It is also known that similar to the IBS of AFP, the fragments of INP have the ability to bind to ice.⁴³ The results of mutation experiments clearly indicate⁴⁴ that INPs organize water molecules in the same way as AFPs but on a much larger scale. Obviously, this is due to the much larger size of INPs and their ability to assemble into aggregates. The large surface area of INP enables a significant increase in the number of HVAs acting as crystallization nuclei, which ultimately translates into the ability to nucleate ice.

MATERIALS AND METHODS

In order to confirm the described model as well as the “fluent clathrate” concept, the following two steps will be required. First, the presence of HVAs and their increased content (compared to bulk water) in the IBS solvation shell of AFP that is NOT located in the vicinity of ice surface have to be confirmed. Second, it has to be demonstrated that the increased HVA content in the IBS solvation water of AFP is directly related to HVA’s ability to bind to the ice surface. The realization of these two steps is the goal of this research. To this end, we selected proteins from the AFP group, differing in both activity and adsorption to different crystallographic planes of ice (*basal* and *prism*). In addition, we also studied the

TABLE I. AFPs investigated in this study.

Protein	PDB code	Antifreeze activity	Protein size (kDa)	Mutation
RiAFP	4DT5	Hyperactive	13.68	...
CfAFP	1LOS	Hyperactive	9.04	...
LpAFP	3ULT	Low	11.32	...
TmAFP	1LII	Hyperactive	8.36	...
ZaAFP	1MSI	Moderate	6.97	...
N14SQ44T	8MSI	Low (10% of wild type)	6.92	ASN14 → SER, GLN44 → THR
T18N	9MSI	Low (10% of wild type)	6.99	THR18 → VAL
T15V	1MSJ	Low (54% of wild type)	6.97	THR15 → ASN

behavior of three different mutants of AFP III (ZaAFP), which were designated as N14SQ44T, T18N, and T15V. The respective activities of these proteins were 10%, 10%, and 54% of native form activity.⁴⁵ The mutations located in the IBS region significantly reduced the antifreeze activity of studied proteins, while the hydrophobic nature of IBS was only slightly affected. Therefore, we found it worthwhile to include those mutants in our study. AFPs investigated in this study are listed in Table I.

The results were obtained with the use of molecular dynamics methods. We conducted computer simulations using the Amber16⁴⁶ package and the ff03 force field in the NpT conditions. The temperatures were kept constant by a Berendsen thermostat.⁴⁷ The pressure of 1 bar was kept constant using the weak coupling method. The lengths of the bonds involving the hydrogen atom were fixed using the SHAKE procedure. The cutoff for nonbonding interactions was equal to 1.2 nm. Equations of motion were integrated with a time step of 2 fs. Periodic boundary conditions were applied for the simulation boxes in all three dimensions. In all simulation systems, the TIP4P/Ice⁴⁸ model of water was used because it has got a freezing temperature that is very close to the experimental value, 272 K.

The 3D structures of AFPs were obtained from the protein data bank. They subsequently solvated in a periodic cubic box of water with at least 2.5 nm from the box walls; the total number of atoms in each molecular system is given in Table I. A certain amount of counterions (Na^+ or Cl^-) were added to neutralize the systems; the ions were restrained at the edge of the box. These counterions were restrained at the edge of the box to avoid their influence on the structure and dynamics of solvation water.⁷ Moreover, the CA atoms of the protein were also restrained at their initial positions. The CA atoms of the protein molecule were restrained using $k_{\text{rest}} = 0.05 \text{ kJ}/(\text{mol} \text{ \AA}^2)$, while ions were restrained using $k_{\text{rest}} = 5.0 \text{ kJ}/(\text{mol} \text{ \AA}^2)$. Initially, ten different, independent copies of each system were prepared, generating initial velocities for each copy from Maxwell distribution. After 1 ns of equilibration at a given temperature, the production simulations were carried out at temperatures of 265, 275, 285, and 298 K. Subsequently, trajectories for analysis were saved every 40 fs. The length of each of the ten independent simulations was equal to 6 ns. Details regarding the methods for the analysis of the results are described in the supplementary material.

RESULTS

When analyzing the properties of solvation water, a number of parameters characterizing its structure was used (for a detailed

description, see the supplementary material). The “differential” method described previously⁴⁹ was employed, which has already allowed precise multiple analyses of the results obtained from simulation runs. A “reference” system was generated by transferring the protein molecules into a separate simulation box filled with liquid water. This procedure is described in detail below, discussing the ordering parameter p used to construct the ordering map.

The IBS, which is responsible for binding of a protein onto ice, displays various structures in different proteins. With the exception of type III proteins (ZaAFP and its mutants), this particular protein region is relatively large, including regular matrix of amino acid residues—this is shown in Fig. S1 in the supplementary material. The IBS of AFP III is relatively small and without any regular pattern of amino acid residues in its structure. Therefore, in the case of AFP III, we assumed the solvation layer covering the entire IBS, while for other AFPs, only the solvation layer of the regular matrix is responsible for binding to ice.

One of the studied proteins, i.e., LpAFP, has an unusual structure, suggesting the existence of two planes that are able to bind to ice.⁵⁰ The mutation experiments clearly showed that only one of the sites is the IBS.⁵¹ However, in our work, we analyzed both regions that had been labeled *side a* (identified as IBS) and *side b*. The non-IBS region of LpAFP covers the remaining fragment of the protein surface, which is outside the *side a* and *side b* regions.

The results of analysis performed on various structural parameters of solvation water, in the temperature range (265–298 K), are presented below. All results refer to the solvation layer with a thickness of 0.45 nm. This value corresponds to the position of the first minimum on the graph showing the distribution of water density as a function of distance from the hydrated surface (see Fig. S2 in the supplementary material).

1. *Preferred positions and orientations of solvation water molecules in the vicinity of IBS.* In order to find preferred positions, we divided the space around the IBS into cubic cells with the length of an edge equal 0.02 nm. We analyzed the degree of occupancy of each cell by the oxygen and hydrogen atoms of water molecules. Based on the constructed histogram, we were able to find and visualize the most likely positions and orientations of water molecules in the vicinity of IBS, as shown in Fig. S3 (see the supplementary material). The tendency to create ring-like structures, formed by water molecules that, we might assume, are probably connected by hydrogen bonds, is noticeable in these pictures. This observation suggests to us an extension of the ACW concept to systems containing AFP molecules surrounded by liquid water under

physiological conditions. We treat the result of this visual assessment as an indication for further investigation path.

2. *Ordering map.* Differences in the structure of solvation water between the two surfaces, i.e., IBS and non-IBS, as well as the structural similarity of the solvation water around the IBS of different proteins, can be clearly observed in the “ordering map.” The concept of this map was taken from the work of DeBenedetti *et al.*^{52,53} The authors proposed that the state of structural ordering can be presented in a diagram, generating the values of two structural ordering parameters of the liquid, i.e., translational and orientational. Esposito *et al.*,⁵⁴ on the other hand, proposed to relate these ordering parameters to a two-particle correlation function. We applied the latter approach in this paper in the following way.

The local ordering parameter p was defined as the following integral of the two-particle correlation function, $g^{(2)}(r, \bar{\omega})$

$$p = -k_B \frac{\rho_W}{16\pi^2} \int_{r=0}^{0.58 \text{ nm}} \int_{\bar{\omega}} \left\{ g^{(2)}(r, \bar{\omega}) \ln [g^{(2)}(r, \bar{\omega}) - g^{(2)}(r, \bar{\omega}) + 1] \right\} r^2 dr d\bar{\omega}, \quad (1)$$

where r represents distance between two water molecules, while $\bar{\omega}$ represents five angles describing their relative orientation. Parameter ρ_W represents the number density of bulk water, while k_B is the Boltzmann constant. As we have shown previously,⁵⁵ this parameter can be decomposed into sum of three terms,

$$p = p_{tra} + p_{con} + p_{ort}, \quad (2)$$

where the individual components p_{tra} , p_{con} , and p_{ort} reflect contributions derived from the translational order (p_{tra} , depending only on the distance between the molecules) and the orientation order (p_{con} and p_{ort} , characterizing the mutual orientation of two adjacent water molecules). We also showed⁵⁵ that the values of the p_{con} and p_{ort} parameters are proportional to each other, so it is possible to use only the p_{con} parameter instead of the sum of $p_{con} + p_{ort}$. This allows for a significant simplification of the calculation procedures. As it results from the definition, the values of all the parameters (p_{tra} , p_{con} , and p_{ort}) are always non-positive: equal to zero in a state of complete disorder (for an ideal gas), and as the degree of order increases, their values become increasingly negative.

The values of parameters $(p_{tra})_{solv}$ and $(p_{con})_{solv}$, determined for the solvation layers of solutes, depend on many factors, such as the thickness and the shape of the analyzed layer as well as the nature of the interaction of water molecules with the solvated surface. The contribution that originates from the latter factor is the most interesting to us because it is what gives the information about the structure of water. However, to assess its magnitude, the influence of other factors needs to be minimized or removed.

To achieve that, we created a “reference” system by transferring the protein molecules into a separate simulation box filled with liquid water (at the same temperature and pressure). By removing the “overlapping” water molecules, we obtain a system in which the introduced protein molecule is surrounded by water with a structure corresponding to bulk water. Determining the values of the parameters $(p_{tra})_{bulk}$ and $(p_{con})_{bulk}$ in the so-defined, fictitious system gives us a point of reference, and the calculated differences in para-

meter values in both systems: $\Delta p_{tra} = (p_{tra})_{solv} - (p_{tra})_{bulk}$ and $\Delta p_{con} = (p_{con})_{solv} - (p_{con})_{bulk}$, reflect the change in the structure of solvation water resulting from its specific interactions with the solvated surface. The values of Δp_{tra} and Δp_{con} obtained in this way determine the position of the point on the “ordering map,” and such a description have been used previously.⁵⁶

Figure 1 shows this map, reflecting changes in the degree of structural ordering of solvation water in relation to bulk water filling the solvation layer.

Two effects are clearly visible in this figure. First, the structure of water around the IBS is different from that surrounding the non-IBS. The sites representing two types of surfaces are clustered in different regions of the map. The second and much more interesting effect is that the temperature variation of the solvation water structure in the two areas, i.e., IBS and non-IBS, is different. For the solvation water of IBS, the difference between the solvation water and bulk water increases steadily as the temperature decreases (both Δp_{tra} and Δp_{con} become more negative). In the case of the solvation water of non-IBS, the opposite trend is observed. The behavior of the solvation water of IBS resembles the pattern obtained previously for the hydration process in model hydrophobic molecules.³⁹ This allows us to suppose that the structural changes in the solvation water around the IBS move toward the formation of the ice-like ordering. Since a characteristic feature of such an ordering is the formation of HVAs, we therefore look for confirmation of the existence of these objects in the solvation water layer. We present these results below.

3. *The average geometry of a single hydrogen bond and the average geometry of the water–water hydrogen bond network in the solvation layer.* HVAs are by definition built of water molecules connected by hydrogen bonds; thus, the geometrical parameters of these bonds are of interest. In this paper, the “conical” definition of hydrogen bonding, proposed by Wernet *et al.*⁵⁷ (see the supplementary material), was used. In order to monitor changes in the geometry of a single bond, a histogram showing the distribution of β -angle values (O–O–H angle) was constructed. Figure 2 presents the differential histogram of $\Delta P(\beta) = P(\beta)_{solv} - P(\beta)_{bulk}$ with noticeable differences between the IBS and non-IBS areas of AFPs studied. The geometry of a single hydrogen bond in the solvation layer around the IBS is closer to being perfect (β -angle closer to zero) compared to bulk water. On the other hand, the geometry of a single hydrogen bond in the solvation layer of the remaining surface area of protein differs only slightly from that in bulk water.

Next, we characterize the geometry of the hydrogen bonding network by taking into account the distribution of ϑ -angle values, where ϑ is the angle between the hydrogen bonds formed by a water molecule with other surrounding water molecules. The “ideal” geometry corresponds to tetrahedral ordering, where the angle ϑ equals 109.5° . Thus, the determined differential histogram of $\Delta P(\vartheta) = P(\vartheta)_{solv} - P(\vartheta)_{bulk}$ reflects the local deformation (relative to the properties of bulk water) of the hydrogen bond network that formed between water molecules in the solvation layer of the analyzed region on the protein surface. In Fig. 2, one can clearly observe an increase in the tetrahedral ordering of water in the vicinity of IBS. At the same time, there is a noticeable decrease in tetrahedral ordering around the non-IBS of the protein molecule, especially at low temperatures (for comparison, see Fig. S4 of the supplementary material). This observation confirms an increase in the “ice-like” ordering of the

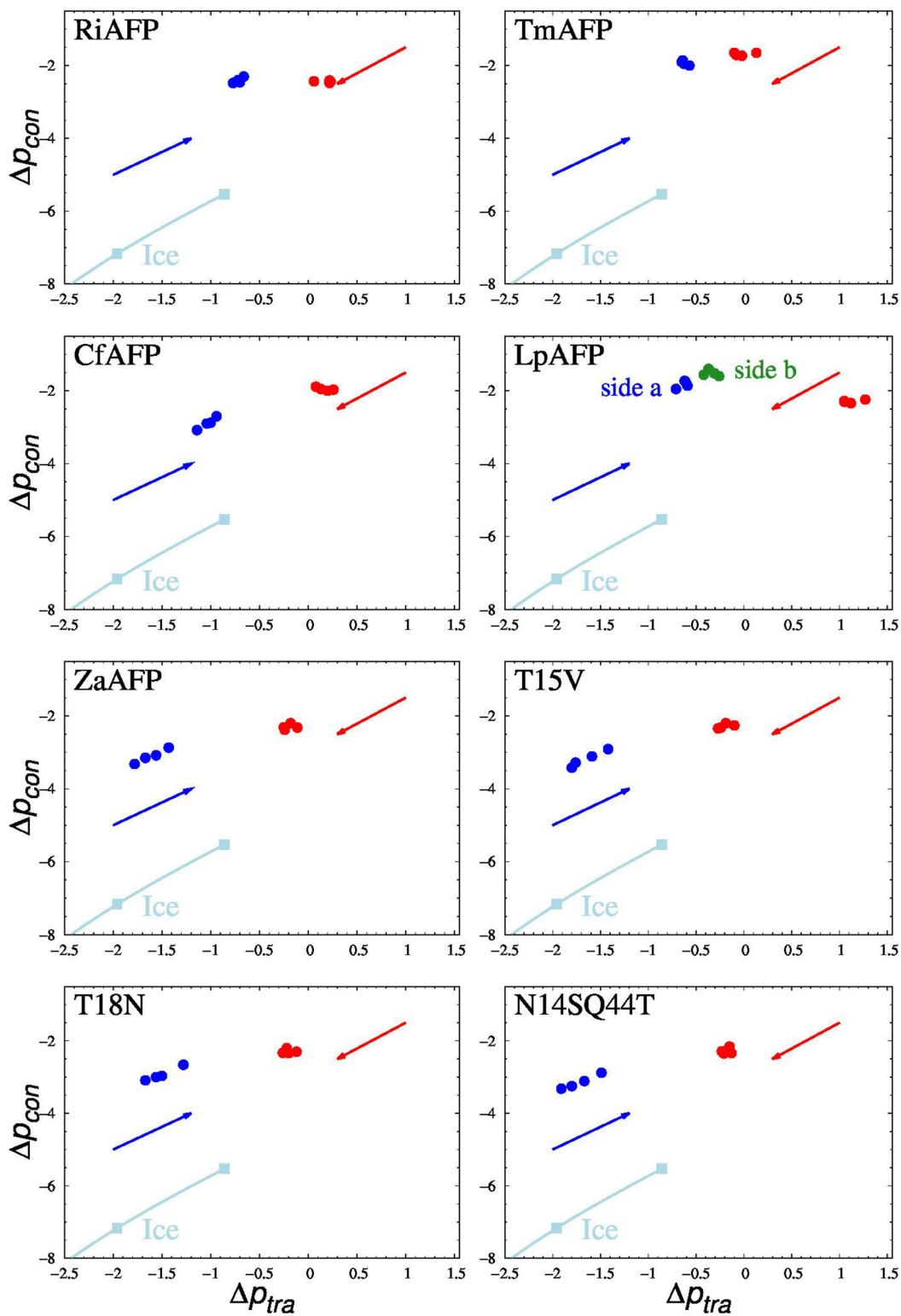


FIG. 1. “Ordering map” (see text), reflecting the structural ordering of solvation water in the vicinity of the IBS (blue points) and non-IBS (red points) areas of the AFPs studied. The arrows on the graph show the direction of change in the location of points on the map with increasing temperature—it is opposite for both areas (IBS and non-IBS). The light-blue line in the graph shows the temperature change in the position of points describing the ordering of the solvation water of the *basal* plane of the ice crystal.

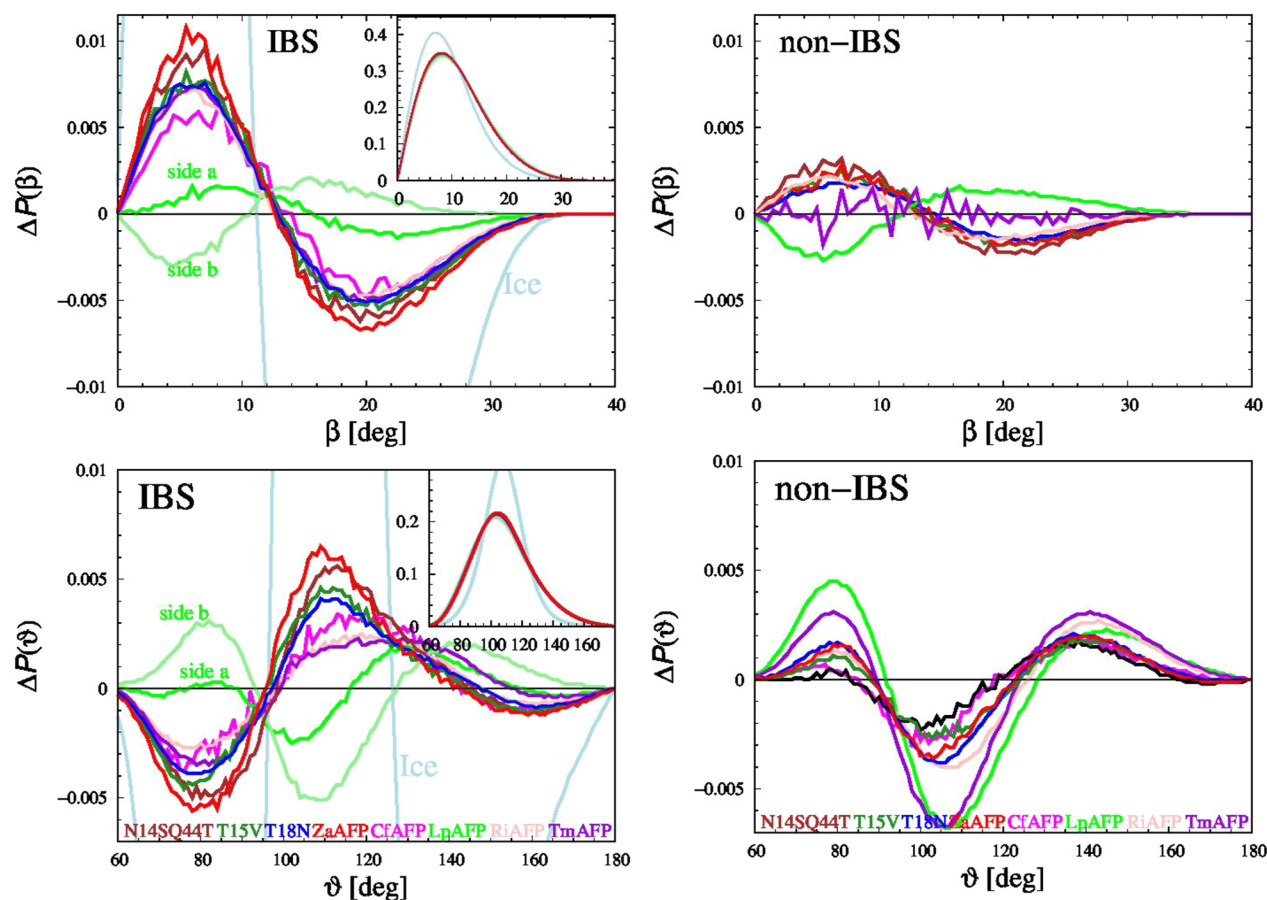


FIG. 2. Comparison of parameters characterizing the average geometry of hydrogen bonds formed by a water molecule contained in the solvation layer of the IBS region and the non-IBS region of the molecules of the considered AFP's. Top row: differential histogram $\Delta P(\beta) = P(\beta)_{\text{solv}} - P(\beta)_{\text{bulk}}$ showing the distribution of β angle values in the water–water hydrogen bond. Bottom row: differential histogram $\Delta P(\vartheta) = P(\vartheta)_{\text{solv}} - P(\vartheta)_{\text{bulk}}$, illustrating the distribution of the values of the ϑ angles—these are the angles between the hydrogen bonds that a water molecule contained in the solvation layer forms with the other surrounding water molecules. The light-blue line illustrates the properties corresponding to the solvation water of the basal plane of the ice crystal. The insets on the graph illustrate the probability distributions for the β and ϑ angles. All the results given at temperature 265 K. Average values of both these angles (β and ϑ) are given in the supplementary material.

solvation water structure around the IBS, which additionally supports the formation of HVAs in this specific water layer.

4. *Analysis of the number of ring structures, formed by water molecules linked by hydrogen bonds, which are contained in the solvation layer.* According to the main assumption regarding the supposed structure of emerging HVAs (see the section titled **Prolegomena**), we analyzed the content of ring structures formed by water molecules via hydrogen bonds in the solvation layer. To assess the tendency to form more complex structures that can be possibly identified as HVAs, we previously³⁹ introduced a parameter τ describing the “compactness” of these structures. The parameter was defined as the ratio of the number of existing five- and six-membered rings in the solvation layer to the total number of water molecules engaged in their formation. A higher parameter value reflects the greater “compactness” of the formed structure. For example, the τ value for a single six-membered ring is 0.167, while for the aforementioned “octameric unit” consisting of three such rings, τ equals

0.375. The average parameter values for the solvation layer, τ_{solv} , are generally in the range (0.35–0.42) and are temperature-dependent. In addition, the τ values for a fictitious solvation layer (filled with bulk water, denoted τ_{bulk}) were calculated in order to compute the $\tau_{\text{solv}}/\tau_{\text{bulk}}$ ratios. As discussed previously,³⁹ it is not the absolute value of $\tau_{\text{solv}}/\tau_{\text{bulk}}$ ratio that is suitable for interpretation, but rather its temperature variation. The values of the ratio increase with decreasing temperature, which indicates that the tendency to form HVAs in the protein solvation layer is increasing (relative to bulk water), as illustrated in Fig. 3. The same effect was observed previously for the molecules of model hydrophobic substances.³⁹ Moreover, it can also be noted that the values of the $\tau_{\text{solv}}/\tau_{\text{bulk}}$ ratio are significantly higher for the solvation water of IBS, which indicates a higher propensity for the HVA formation around the IBS compared to the non-IBS. Thus, the presented results directly confirm the tendency to form HVAs in the solvation layer surrounding the IBS in all studied AFPs.

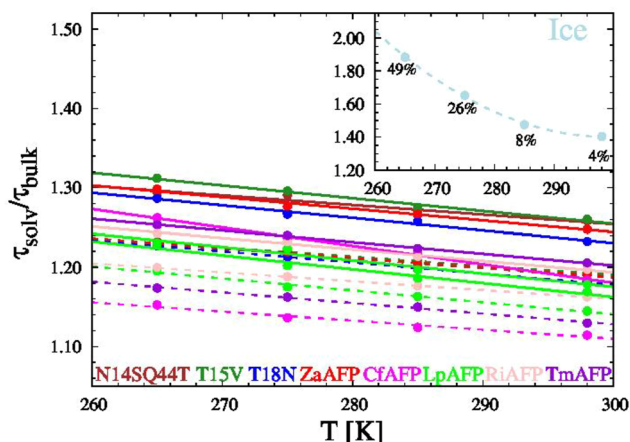


FIG. 3. The values of the τ_{solv}/τ_{bulk} ratio, determined for water within the solvation layer of the surface of IBS and non-IBS AFP molecules. The solid lines describe IBS, and the dashed lines describe non-IBS. In the inset, we have included the temperature dependence of the value of the τ_{solv}/τ_{bulk} ratio determined for water within the solvation layer of the basal plane of ice; the numbers next to the points on the graph give the (percentage) ice content of the solvation layer, as determined by the CHILL+ algorithm.⁵⁸

5. *Direct confirmation of the existence of “locally favored structures” in the solvation layer using dedicated parameters.* Russo and Tanaka^{35,59,60} recently introduced parameter ζ , which is defined as “...the difference between the distance $d_{j'i}$ of the closest neighbor molecule j' not H-bonded to molecule i and the distance $d_{j''i}$ of the furthest neighbor molecule j'' H-bonded to molecule i : $\zeta(i) = d_{j'i} - d_{j''i}$.”⁵⁹ This parameter was designed specifically to identify “locally favored structures” in liquid water. Using the description presented in the section titled **Prolegomena**, we currently identify the “locally favored structures” described by Tanaka as HVAs.

As shown by Tanaka, the distribution of ζ values is bimodal, with the maxima of its two modes located approximately at zero and 0.08 nm.³⁵ The mode located at 0.08 nm reflects the presence of “locally favored structures” (i.e., HVA) in water.^{35,59,60} As in the case of other parameters discussed above, the ζ values were determined twice, i.e., first, for the solvation layer of the protein molecule and, second, for a fictitious solvation layer filled with bulk water. The differential histogram of $\Delta P(\zeta) = P(\zeta)_{solv} - P(\zeta)_{bulk}$, shown in Fig. 4, reflects the change in the tendency to form HVAs in the solvation water layer in comparison to bulk water. The preference for the formation of “locally favored structures” (i.e., the HVA structures) in the vicinity of IBS as well as the propensity for their disorganization around the non-IBS was very evident in all studied proteins.

LSI (local structure index) is another parameter, methodologically similar to ζ . LSI is a measure of heterogeneity of radial distribution of water molecules within short distances (up to about 0.37 nm). It was defined by Shiratani and Sasai^{61,62} as follows: For each water molecule i , the rest of the water molecules is ordered depending on the radial distance r_j between the oxygen atom of the molecule i and the oxygen atom of molecule j : $r_1 < r_2 < \dots < r_j < \dots < r_n < r_{n+1}$, while n is chosen so that $r_n < 0.37 \text{ nm} < r_{n+1}$. Then, LSI is defined as^{61,62}

$$LSI = \frac{1}{n} \sum_{j=1}^n [\Delta(j) - \bar{\Delta}]^2, \quad (3)$$

where $\Delta(j) = r_{j+1} - r_j$ and $\bar{\Delta}$ is the average value of $\Delta(j)$ (over all molecules). Since it was introduced, it has been used, among others, to demonstrate that the two phases of different densities coexist in supercooled liquid water, i.e., high density amorphous phase, HDA, and low density amorphous phase, LDA.^{63,64} As in the case of ζ , the distribution of LSI values is also bimodal, where higher parameter values correspond to higher HVA content in liquid water.^{63,64}

The calculated differential histogram of $\Delta P(LSI) = P(LSI)_{solv} - P(LSI)_{bulk}$, depicted in Fig. 4, reveals the shape distribution, which confirms both the tendency to form HVAs in the solvation water of IBS and the disorganization of these structures in the vicinity of other areas on the surface of analyzed proteins. Therefore, the analysis of the two described parameters (i.e., ζ and LSI) provides direct evidence of increased HVA content in the solvation water around the IBS and reduced HVA content in the vicinity of the remaining areas on the surface of proteins.

6. *The increased probability of HVA formation in the solvation layer of IBS is a necessary but not sufficient condition for AFP functionality.* The results presented above allow us to conclude that the formation of “fluent clathrates” occurs only in the solvation water around the IBS of the AFP molecule, while in the vicinity of the non-IBS region, HVAs are partially destructed. The HVA destruction can explain the well-known observation^{5,6} about water contained in the solvation layer of “ordinary” protein molecules not being able to transform into ice. In turn, the weakening of the tendency to form HVAs around the IBS on the LpAFP surface results in a significant reduction in the antifreeze activity of the protein (the highest measurable value of the width of the hysteresis loop for LpAFP is 0.1 °C, while for hyperactive insect AFPs, it is 5–6 °C⁶⁵). This finding unquestionably indicates that shifting the equilibrium toward the HVA formation in the solvation water of IBS and the consequent binding of formed HVAs to the IBS (thus the existence of “fluent clathrate,” as described by us) is a prerequisite for AFP functionality, at least for AFPs having a well-defined IBS region.

On the other hand, however, the analysis carried out for AFP III and its mutants clearly shows that the structure of solvation water around the IBS in all these molecules (i.e., ZaAFP and its mutants) is very similar. The introduced mutations significantly (up to tenfold) reduce antifreeze activity of protein, which proves that the formation of described “fluent clathrate” is a necessary but not sufficient condition to ensure this activity. Thus, it would be useful to explain the evident reduction in antifreeze activity of these mutants in comparison to wild type. In this context, the concepts presented by Knight and Wierzbicki⁶⁶ are helpful. The authors listed “resistance to rejection” as one of the criteria determining antifreeze activity in a protein; this parameter reflects, to some extent, the binding strength of the AFP molecule to the ice surface. In our proposed model, this would correspond to the number of sites (e.g., OH groups) at which nascent HVA binds to the IBS. Reducing the number of such “hot” spots, or even just changing their arrangement on the IBS in such a manner as to hinder the transformation of HVAs into ice cells, will result in a decrease in the binding strength of IBS to the ice surface. Consequently, this will facilitate detachment of AFP from the ice surface, reducing the activity of the protein. This phenomenon has been confirmed by the results recently reported

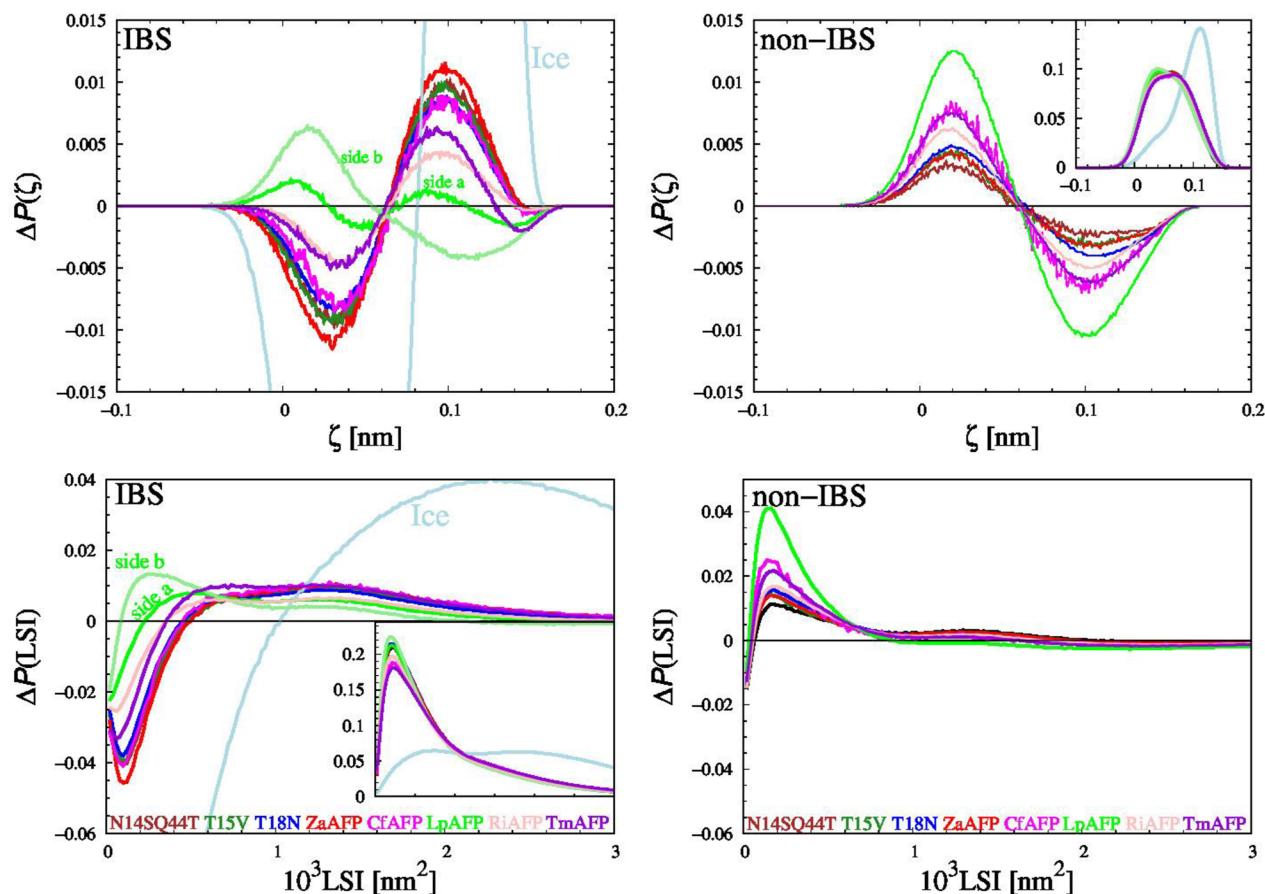


FIG. 4. Top row: differential histogram $\Delta P(\zeta) = P(\zeta)_{\text{sol}} - P(\zeta)_{\text{bulk}}$, showing the distribution of values of the ζ parameter, reflecting the tendency to form HVA in solvation water of different areas (IBS and non-IBS) on the surface of the AFP molecules studied. The bottom row illustrates the analogous distribution for the LSI parameter. The insets in the graph illustrate the probability distributions of both parameters (ζ and LSI). The light-blue line illustrates the properties corresponding to the solvation water of the basal plane of the ice crystal. All the results are given at a temperature of 265 K.

by Kumari *et al.*⁶⁷ The authors studied adsorption of ZaAFP and mutant T18N (10% activity of wild type) on the ice surface. The increased detachment probability of T18N molecule (compared to wild type) at the ice–water interface was observed, which reached 0.20 and 0.50 for wild type and T18N mutant, respectively.

CONCLUSIONS

The purpose of this study was to confirm the correctness of “fluent clathrate” concept as well as to demonstrate that the formation of such a clathrate is a prerequisite for the binding of AFP to ice. Following other authors,^{28,29,32} we started with the assumption that in liquid water, there is a natural tendency to form HVAs, which are composed of water molecules linked by hydrogen bonds. Such spontaneously formed HVAs are surrounded by a “sea” of disordered water molecules, where both forms are in equilibrium. We also assumed that the same process of HVA formation takes place in the solvation water, although in this case, the tendency to form HVAs is modified by the interactions of water molecules with the protein surface. In other words, these interactions can shift the equilibrium

point of HVA formation. The results of analysis performed by using various parameters characterizing the solvation water structure fully confirm the above assumptions. Formation of HVAs and the dependence of HVA content in the solvation water on the characteristic of solvated surface were demonstrated. In comparison to bulk water, a significantly higher HVA presence in the water layer around the IBS of AFP was observed, while in the vicinity of non-IBS, the probability of HVA formation was significantly lower. The spontaneously formed HVAs underwent partial destruction in solvation water due to interaction with non-IBS. The aforementioned greater tendency to form HVAs in the vicinity of IBS is due to the hydrophobic nature of this surface. On the other hand, the presence of OH groups on the IBS enables HVAs to bind to this surface, which seems to additionally stabilize the formed aggregates (similar to what occurs in the solvation water of ice). Because the HVAs formed in liquid water do not have a strictly defined, in the crystallographic sense, spatial structure, thus, we propose²⁷ a term “fluent clathrate” for the set of HVAs “anchored” in this way. This name is in line with the term “anchored clathrate” proposed by Garnham *et al.*¹³ as it emphasizes that each HVA has a certain ordered internal structure, i.e.,

the mutual positions and orientations of water molecules are not random. On the other hand, the word “fluent” emphasizes that the structure is somewhat blurred and changes over time.

When the IBS of an AFP is close to the surface of a growing ice crystal (at a distance of *ca.* one nm or less), the solvation layers of IBS and ice overlap. This affects the process of water solidification in the space between the IBS and ice surface. The transformation of liquid water into ice is a relatively slow process (on a molecular scale) that involves gradual reorganization of liquid's structure toward an increase in HVA content. Smaller HVAs merge into larger aggregates,^{32,40} and because they display a high degree of orientational ordering, the structure of liquid water becomes ice-like. In this way, an ice-like lattice gradually builds up in the water. The higher the HVA content in a liquid, the greater its tendency to transform into ice. Thus, it can be concluded that under the above mentioned conditions (the AFP molecule is close to the surface of a growing ice crystal), HVAs in a liquid act as nascent ice nuclei. Such an explanation of changes in the structure of water during the solidification process allows us to avoid the controversial use of the phrase “ice-like structure of water” as encountered in the literature. Thus, if the IBS of AFP is located close to the ice surface, then the structural reorganization of solvation water is dictated by the structural compatibility of HVAs present in two overlapping solvation shells, i.e., surrounding the IBS and ice surface. We previously²⁷ presented a detailed description of this transformation occurring over time. The process was also observed by Hudait *et al.*,¹⁷ who interpreted it as follows: the ACW motif forms only when the AFP molecule moves into the vicinity of ice surface and positions itself in an orientation optimal for binding to ice. We postulate a different interpretation, i.e., a gradual rearrangement of the existing “ice-like” structure of “fluent clathrate” during the solidification process, which ultimately leads to the formation of a solid phase (ice).

SUPPLEMENTARY MATERIAL

The supplementary material includes a description of the technical details of the calculations (range of the solvation shell, definition of hydrogen bond, and ring analysis) and also an illustration of the most probable orientations and positions of solvation water molecules in the vicinity of the IBS of the studied protein molecules. The attached table also includes geometrical characteristics of the water–water hydrogen bonding network that is formed between water molecules contained in the solvation layer of the studied proteins.

ACKNOWLEDGMENTS

The author would like to thank Dr. Joanna Grabowska for preparing the starting files for computer simulations. This research was supported, in part, by PL-Grid Infrastructure. The calculations were carried out at the Academic Computer Center (TASK) in Gdańsk.

AUTHOR DECLARATIONS

Conflict of Interest

The author has no conflicts to disclose.

Author Contributions

Jan Zielkiewicz: Conceptualization (equal); Formal analysis (equal); Investigation (equal); Methodology (equal); Writing – original draft (equal).

DATA AVAILABILITY

The data that support the findings of this study are available from the corresponding author upon reasonable request.

REFERENCES

- Y. Celik, L. A. Graham, Y.-F. Mok, M. Bar, P. L. Davies, and I. Braslavsky, “Superheating of ice crystals in antifreeze protein solutions,” *Proc. Natl. Acad. Sci. U. S. A.* **107**, 5423–5428 (2010).
- Y. Celik, R. Drori, N. Pertaya-Braun, A. Altan, T. Barton, M. Bar-Dolev, A. Groisman, P. L. Davies, and I. Braslavsky, “Microfluidic experiments reveal that antifreeze proteins bound to ice crystals suffice to prevent their growth,” *Proc. Natl. Acad. Sci. U. S. A.* **110**, 1309–1314 (2013).
- R. Drori, P. L. Davies, and I. Braslavsky, “When are antifreeze proteins in solution essential for ice growth inhibition?,” *Langmuir* **31**, 5805–5811 (2015).
- E. Kristiansen and K. E. Zachariassen, “The mechanism by which fish antifreeze proteins cause thermal hysteresis,” *Cryobiology* **51**, 262–280 (2005).
- K. Tompa, P. Bánki, M. Bokor, P. Kamasa, G. Lasanda, and P. Tompa, “Interfacial water at protein surfaces: Wide-line NMR and DSC characterization of hydration in ubiquitin solutions,” *Biophys. J.* **96**, 2789–2798 (2009).
- A. B. Siemer, K.-Y. Huang, and A. E. McDermott, “Protein–ice interaction of an antifreeze protein observed with solid-state NMR,” *Proc. Natl. Acad. Sci. U. S. A.* **107**, 17580–17585 (2010).
- J. Grabowska, A. Kuffel, and J. Zielkiewicz, “Molecular dynamics study on the role of solvation water in the adsorption of hyperactive AFP to the ice surface,” *Phys. Chem. Chem. Phys.* **20**, 25365–25376 (2018).
- N. Smolin and V. Daggett, “Formation of ice-like water structure on the surface of an antifreeze protein,” *J. Phys. Chem. B* **112**, 6193–6202 (2008).
- D. R. Nutt and J. C. Smith, “Dual function of the hydration layer around an antifreeze protein revealed by atomistic molecular dynamics simulations,” *J. Am. Chem. Soc.* **130**, 13066–13073 (2008).
- Y. Xu, R. Gnanasekaran, and D. M. Leitner, “Analysis of water and hydrogen bond dynamics at the surface of an antifreeze protein,” *J. At. Mol. Phys.* **2012**, 125071.
- K. Meister, S. Ebbinghaus, Y. Xu, J. G. Duman, A. DeVries, M. Gruebele, D. M. Leitner, and M. Havenith, “Long-range protein–water dynamics in hyperactive insect antifreeze proteins,” *Proc. Natl. Acad. Sci. U. S. A.* **110**, 1617–1622 (2013).
- K. Meister, S. Strazdaite, A. L. DeVries, S. Lotze, L. L. C. Olijve, I. K. Voets, and H. J. Bakker, “Observation of ice-like water layers at an aqueous protein surface,” *Proc. Natl. Acad. Sci. U. S. A.* **111**, 17732–17736 (2014).
- C. P. Garnham, R. L. Campbell, and P. L. Davies, “Anchored clathrate waters bind antifreeze proteins to ice,” *Proc. Natl. Acad. Sci. U. S. A.* **108**, 7363–7367 (2011).
- K. A. Sharp, “A peek at ice binding by antifreeze proteins,” *Proc. Natl. Acad. Sci. U. S. A.* **108**, 7281–7282 (2011).
- A. J. Middleton, C. B. Marshall, F. Faucher, M. Bar-Dolev, I. Braslavsky, R. L. Campbell, V. K. Walker, and P. L. Davies, “Antifreeze protein from freeze-tolerant grass has a beta-roll fold with an irregularly structured ice-binding site,” *J. Mol. Biol.* **416**, 713–724 (2012).
- N. M.-M. U. Khan, T. Arai, S. Tsuda, and H. Kondo, “Characterization of microbial antifreeze protein with intermediate activity suggests that a bound-water network is essential for hyperactivity,” *Sci. Rep.* **11**, 5971 (2021).
- A. Hudait, D. R. Moberg, Y. Qiu, N. Odendahl, F. Paesani, and V. Molinero, “Preordering of water is not needed for ice recognition by hyperactive antifreeze proteins,” *Proc. Natl. Acad. Sci. U. S. A.* **115**, 8266–8271 (2018).

- ¹⁸K. Modig, J. Qvist, C. B. Marshall, P. L. Davies, and B. Halle, "High water mobility on the ice-binding surface of a hyperactive antifreeze protein," *Phys. Chem. Chem. Phys.* **12**, 10189–10197 (2010).
- ¹⁹E. Duboué-Dijon and D. Laage, "Comparative study of hydration shell dynamics around a hyperactive antifreeze protein and around ubiquitin," *J. Chem. Phys.* **141**, 22D529 (2014).
- ²⁰S. Cui, W. Zhang, X. Shao, and W. Cai, "Hyperactive antifreeze proteins promote ice growth before binding to it," *J. Chem. Inf. Model.* **62**, 5165 (2021).
- ²¹S. Cui, W. Zhang, X. Shao, and W. Cai, "Do antifreeze proteins generally possess the potential to promote ice growth?" *Phys. Chem. Chem. Phys.* **24**, 7901–7908 (2022).
- ²²O. A. Karim and A. D. J. Haymet, "The ice/water interface: A molecular dynamics simulation study," *J. Chem. Phys.* **89**, 6889–6896 (1988).
- ²³D. Beaglehole and P. Wilson, "Thickness and anisotropy of the ice-water interface," *J. Phys. Chem.* **97**, 11053–11055 (1993).
- ²⁴M. M. Conde, C. Vega, and A. Patrykiewicz, "The thickness of a liquid layer on the free surface of ice as obtained from computer simulation," *J. Chem. Phys.* **129**, 014702 (2008).
- ²⁵S. Chakraborty and B. Jana, "Ordered hydration layer mediated ice adsorption of a globular antifreeze protein: Mechanistic insight," *Phys. Chem. Chem. Phys.* **21**, 19298–19310 (2019).
- ²⁶S. Chakraborty and B. Jana, "Molecular insight into the adsorption of Spruce budworm antifreeze protein to an ice surface: A clathrate-mediated recognition mechanism," *Langmuir* **33**, 7202–7214 (2017).
- ²⁷J. Grabowska, A. Kuffel, and J. Zielkiewicz, "Interfacial water controls the process of adsorption of hyperactive antifreeze proteins onto the ice surface," *J. Mol. Liq.* **306**, 112909 (2020).
- ²⁸G. Némethy and H. A. Scheraga, "Structure of water and hydrophobic bonding in proteins. I. A model for the thermodynamic properties of liquid water," *J. Chem. Phys.* **36**, 3382–3400 (1962).
- ²⁹H. Tanaka, "Simple physical model of liquid water," *J. Chem. Phys.* **112**, 799–809 (2000).
- ³⁰O. Mishima and H. E. Stanley, "The relationship between liquid, supercooled and glassy water," *Nature* **396**, 329–335 (1998).
- ³¹H. Tanaka, "Simple physical explanation of the unusual thermodynamic behavior of liquid water," *Phys. Rev. Lett.* **80**, 5750–5753 (1998).
- ³²F. H. Stillinger, "Water revisited," *Science* **209**, 451–457 (1980).
- ³³H. Tanaka, "Thermodynamic anomaly and polyamorphism of water," *Europhys. Lett.* **50**, 340–346 (2000).
- ³⁴H. Tanaka, "Two-order-parameter description of liquids. I. A general model of glass transition covering its strong to fragile limit," *J. Chem. Phys.* **111**, 3163–3174 (1999).
- ³⁵J. Russo and H. Tanaka, "Understanding water's anomalies with locally favoured structures," *Nat. Commun.* **5**, 3556 (2014).
- ³⁶A. Kuffel and J. Zielkiewicz, "Why the solvation water around proteins is more dense than bulk water," *J. Phys. Chem. B* **116**, 12113–12124 (2012).
- ³⁷A. D. J. Haymet, L. G. Ward, and M. M. Harding, "Winter flounder 'antifreeze' proteins: Synthesis and ice growth inhibition of analogues that probe the relative importance of hydrophobic and hydrogen-bonding interactions," *J. Am. Chem. Soc.* **121**, 941–948 (1999).
- ³⁸H. S. Frank and M. W. Evans, "Free volume and entropy in condensed systems III. Entropy in binary liquid mixtures; partial molal entropy in dilute solutions; structure and thermodynamics in aqueous electrolytes," *J. Chem. Phys.* **13**, 507–532 (1945).
- ³⁹J. Grabowska, A. Kuffel, and J. Zielkiewicz, "Revealing the Frank–Evans 'iceberg' structures within the solvation layer around hydrophobic solutes," *J. Phys. Chem. B* **125**, 1611–1617 (2021).
- ⁴⁰H. Tanaka, "General view of a liquid-liquid phase transition," *Phys. Rev. E* **62**, 6968–6976 (2000).
- ⁴¹K. Mochizuki and M. Matsumoto, "Collective transformation of water between hyperactive antifreeze proteins: RiAFPs," *Crystals* **9**, 188 (2019).
- ⁴²C. P. Garnham, R. L. Campbell, V. K. Walker, and P. L. Davies, "Novel dimeric β -helical model of an ice nucleation protein with bridged active sites," *BMC Struct. Biol.* **11**, 36 (2011).
- ⁴³Y. Kobashigawa, Y. Nishimiya, K. Miura, S. Ohgiya, A. Miura, and S. Tsuda, "A part of ice nucleation protein exhibits the ice-binding ability," *FEBS Lett.* **579**, 1493–1497 (2005).
- ⁴⁴J. Forbes, A. Bissoyi, L. Eickhoff, N. Reicher, T. Hansen, C. G. Bon, V. K. Walker, T. Koop, Y. Rudich, I. Braslavsky, and P. L. Davies, "Water-organizing motif continuity is critical for potent ice nucleation protein activity," *Nat. Commun.* **13**, 5019 (2022).
- ⁴⁵S. P. Graether, C. I. DeLuca, J. Baardsnes, G. A. Hill, P. L. Davies, and Z. Jia, "Quantitative and qualitative analysis of type III antifreeze protein structure and function," *J. Biol. Chem.* **274**, 11842–11847 (1999).
- ⁴⁶D. A. Case, R. Betz, D. S. Cerutti, T. E. Cheatham, T. A. Darden, R. E. Duke, T. Giese, H. Gohlke, A. W. Goetz, N. Homeyer, S. Izadi, P. Janowski, J. Kaus, A. Kovalenko, T. S. Lee, S. LeGrand, P. Li, C. Lin, T. Luchko, R. Luo, B. Madej, D. Mermelstein, K. M. Merz, G. Monard, H. Nguyen, H. T. Nguyen, I. Omelyan, A. Onufriev, D. R. Roe, A. Roitberg, C. Sagui, C. L. Simmerling, W. M. Botello-Smith, J. Swails, R. C. Walker, J. Wang, R. M. Wolf, X. Wu, L. Xiao, and P. A. Kollman, *Amber 16*, University of California, San Francisco, 2016.
- ⁴⁷H. J. C. Berendsen, J. P. M. Postma, W. F. van Gunsteren, A. DiNola, and J. R. Haak, "Molecular dynamics with coupling to an external bath," *J. Chem. Phys.* **81**, 3684–3690 (1984).
- ⁴⁸J. L. F. F. Abascal, E. Sanz, R. García Fernández, C. Vega, R. G. Fernández, and C. Vega, "A potential model for the study of ices and amorphous water: TIP4P/Ice," *J. Chem. Phys.* **122**, 234511 (2005).
- ⁴⁹A. Kuffel and J. Zielkiewicz, "The importance of the shape of the protein–water interface of a kinesin motor domain for dynamics of the surface atoms of the protein," *Phys. Chem. Chem. Phys.* **14**, 5561–5569 (2012).
- ⁵⁰M. J. Kuiper, P. L. Davies, and V. K. Walker, "A theoretical model of a plant antifreeze protein from *Lolium perenne*," *Biophys. J.* **81**, 3560–3565 (2001).
- ⁵¹A. J. Middleton, A. M. Brown, P. L. Davies, and V. K. Walker, "Identification of the ice-binding face of a plant antifreeze protein," *FEBS Lett.* **583**, 815–819 (2009).
- ⁵²T. M. Truskett, S. Torquato, and P. G. Debenedetti, "Towards a quantification of disorder in materials: Distinguishing equilibrium and glassy sphere packings," *Phys. Rev. E* **62**, 993–1001 (2000).
- ⁵³J. R. Errington and P. G. Debenedetti, "Relationship between structural order and the anomalies of liquid water," *Nature* **409**, 318–321 (2001).
- ⁵⁴R. Esposito, F. Saija, A. Marco Saitta, and P. V. Giaquinta, "Entropy-based measure of structural order in water," *Phys. Rev. E* **73**, 040502 (2006).
- ⁵⁵J. Zielkiewicz, "Two-particle entropy and structural ordering in liquid water," *J. Phys. Chem. B* **112**, 7810–7815 (2008).
- ⁵⁶A. Kuffel, D. Czapiewski, and J. Zielkiewicz, "Unusual structural properties of water within the hydration shell of hyperactive antifreeze protein," *J. Chem. Phys.* **141**, 055103 (2014).
- ⁵⁷P. Wernet, D. Nordlund, U. Bergmann, M. Cavalleri, M. Odelius, H. Ogasawara, L. A. Näslund, T. K. Hirsch, L. Ojamäe, P. Glatzel, L. G. M. Pettersson, and A. Nilsson, "The structure of the first coordination shell in liquid water," *Science* **304**, 995–999 (2004).
- ⁵⁸A. H. Nguyen and V. Molinero, "Identification of clathrate hydrates, hexagonal ice, cubic ice, and liquid water in simulations: The CHILL+ algorithm," *J. Phys. Chem. B* **119**, 9369–9376 (2015).
- ⁵⁹R. Shi, J. Russo, and H. Tanaka, "Common microscopic structural origin for water's thermodynamic and dynamic anomalies," *J. Chem. Phys.* **149**, 224502 (2018).
- ⁶⁰R. Shi and H. Tanaka, "Microscopic structural descriptor of liquid water," *J. Chem. Phys.* **148**, 124503 (2018).
- ⁶¹E. Shiratani and M. Sasai, "Growth and collapse of structural patterns in the hydrogen bond network in liquid water," *J. Chem. Phys.* **104**, 7671–7680 (1996).
- ⁶²E. Shiratani and M. Sasai, "Molecular scale precursor of the liquid–liquid phase transition of water," *J. Chem. Phys.* **108**, 3264–3276 (1998).
- ⁶³G. A. Appignanesi, J. A. Rodriguez Fris, and F. Sciortino, "Evidence of a two-state picture for supercooled water and its connections with glassy dynamics," *Eur. Phys. J. E* **29**, 305–310 (2009).

⁶⁴S. R. Accordino, J. A. Rodriguez Fris, F. Sciortino, and G. A. Appignanesi, "Quantitative investigation of the two-state picture for water in the normal liquid and the supercooled regime," *Eur. Phys. J. E* **34**, 48 (2011).

⁶⁵C. Sidebottom, S. Buckley, P. Pudney, S. Twigg, C. Jarman, C. Holt, J. Telford, A. McArthur, D. Worrall, R. Hubbard, and P. Lillford, "Heat-stable antifreeze protein from grass," *Nature* **406**, 256 (2000).

⁶⁶C. A. Knight and A. Wierzbicki, "Adsorption of biomolecules to ice and their effects upon ice growth. 2. A discussion of the basic mechanism of 'antifreeze' phenomena," *Cryst. Growth Des.* **1**, 439–446 (2001).

⁶⁷S. Kumari, A. V. Muthachikavil, J. K. Tiwari, and S. N. Punnathanam, "Computational study of differences between antifreeze activity of type-III antifreeze protein from ocean pout and its mutant," *Langmuir* **36**, 2439–2448 (2020).